Impact of stochastic physics on tropical precipitation in the coupled ECMWF model

Aneesh Subramanian[a] *, Antje Weisheimer [b,c], Tim Palmer [a], Frederic Vitart [c] and Peter Bechtold [c]

[a]*Department of Physics, University of Oxford, Oxford*

[b] *Department of Physics, National Centre for Atmospheric Science (NCAS), University of Oxford, Oxford*

[c] *European Centre for Medium-Range Weather Forecasts (ECMWF), Reading, UK*

*Correspondence to: Department of Physics, University of Oxford, Oxford - OX1 3PU. email: subramanian@atm.ox.ac.uk

Uncertainties in parameterized processes in general circulation models can be represented as stochastic perturbations to the model formulation. The European Centre for Medium-Range Weather Forecasts (ECMWF) has pioneered approaches to represent these model errors in forecasting systems. In particular, the stochastically perturbed physical tendency (SPPT) scheme for the atmosphere is used in their operational ensemble system for medium- and long-range predictions. Recent studies have shown that these stochastic approaches can both increase the reliability of the probabilistic forecasts and reduce long-term mean biases of the model climate. Towards developing a seamless prediction system in the future, these benefits of stochastic parameterization for both short-term and long-term forecasts make it an essential component of the next generation Earth System Models. We present results of the impact of different configurations of the SPPT scheme in ECMWF's seasonal forecasting System 4 on the mean and variability in tropical precipitation. Small scale perturbations in the SPPT scheme play a significant role in reducing the mean biases in tropical precipitation. The stochastic physics also non-linearly rectifies the convection and precipitation during different phases of El Niño Southern Oscillation events and improves the reliability of the ensemble forecasts for the Madden-Julian Oscillation (MJO). They impact the MJO dynamics by modulating the convective and suppressed phases of the MJO. Finally, we discuss some of the caveats to this analysis and some future prospects.

Key Words: Stochastic Physics, SPPT, MJO, ENSO, ITCZ

Received . . .

1. Introduction

Atmospheric convection plays a key role in regulating the climate in the Tropics (Bony *et al.* 2015), and is one of the most challenging processes to parameterize in weather and climate models. Inadequate representation of convection in weather and climate prediction models leads to the largest uncertainties in forecasts especially in aspects related to the hydrological cycle in the Tropics (Brunet *et al.* 2010). Many scientific and technological advances have led to increasing the forecast skill of operational weather forecasting models on timescales of upto two weeks over the past five decades (Bauer *et al.* 2015). Progress has also been made in seasonal climate predictions (Brunet *et al.* 2010), yet the current challenge lies in bringing the communities of weather and climate together to address issues with predictability on subseasonal-to-seasonal and longer timescales (Vitart and Robertson 2012). Past experience and some theoretical studies have shown that the predictability of daily weather cannot be extended beyond the two week period, even if we reduce the initial error on subsynoptic scales, but larger than the scales of viscous dissipation (Durran and Gingrich 2014; Palmer *et al.* 2014). Yet, slowly evolving boundary and forcing conditions of the atmosphere can lead to predictability on timescales beyond couple of weeks and longer for some modes of climate variability (Pegion and Sardeshmukh 2011; Vitart and Robertson 2012; Vitart 2014; Robertson *et al.* 2015).

Tropical convection shows a remarkable amount of variability across many spatial and temporal scales, ranging from individual convective clouds to mesoscale and synoptic-scale organized convection. The key barriers in our capability to predict the tropical precipitation on timescales of weather to climate are partly due to the lack in knowledge of convective processes that impact predictability at these timescales and partly due to ill-represented convective processes in our earth system models (Moncrieff *et al.* 2007).

The power-law spectra of atmospheric dynamics implies that there is no accurate way to separate dynamics on resolved scales and unresolved scales in a weather or climate model. Hence, errors in very small scales can propagate upscale and generate errors in the large-scale flow in finite time. The propagation of such uncertainties in both initial conditions and model formulation translate into limits on predictability of weather and climate forecasts (Palmer and Williams 2008). Since it is essential to be able to estimate the impact of such uncertainties on forecast accuracy, no weather or climate prediction can be considered complete without a forecast of the associated flow-dependent predictability. Also our ability to provide reliable weather and climate predictions and the concomitant uncertainty associated with the predicted fields is vital for robust decision making across many different socio-economic applications. Hence, representing uncertainty in convective and other physical parameterization in weather and climate models is necessary for an improved probabilistic forecast system.

The major sources of uncertainties for weather forecasts are in the initial conditions and in the model error, while for climate forecasts the initial uncertainties play less of a role in projecting on to forecast uncertainties. On timescales of less than a week the initial uncertainty may play a more dominant role than the model uncertainty while on subseasonal-to-seasonal timescales both these sources of uncertainties play key roles in the propagation of the forecast uncertainty. Practically, the problem of integrating the uncertainties in forecasts is addressed by using ensembles of integrations of comprehensive weather and climate prediction models, first suggested by Leith (1975), with explicit perturbations to both initial conditions and model formulation. Forecasts resulting from such an ensemble system can be thought as probabilistic forecasts representing the probabilities of integrated fields in an approximate way.

One approach for simulating perturbations to model formulation is stochastic parameterisation of the physical tendencies in the forecast system. A more detailed motivation for including stochastic parameterisations in our current weather and climate models is presented in Palmer (2012). Successful applications of stochastic approaches in numerical weather prediction (NWP) have evolved in the recent decade from the early attempts in the European Centre for Medium-Range Weather Forecasts (ECMWF) ensemble prediction system (Palmer *et al.* 1997) to operational schemes at several meteorological services around the world to make ensemble predictions from short-range to seasonal time scales (Teixeira and Reynolds 2010; Reyes *et al.* 2009; Berner *et al.*

2010; Stockdale *et al.* 2011; Palmer *et al.* 2009b; Palmer 2012; Suselj *et al.* 2013; Sušelj *et al.* 2014; Sanchez *et al.* 2015). The currently operational medium-range ensemble prediction system at ECMWF includes two schemes to represent model uncertainty, the stochastically perturbed physical tendencies (SPPT) scheme and the stochastically perturbed backscatter (SPBS) scheme. The SPPT scheme is based on the Buizza *et al.* (1999) scheme and applies stochastic perturbations in the form of multiplicative noise to the diabatic (parametrized) part of the tendency equations of the prognostic variables (Palmer *et al.* 2009a; Weisheimer *et al.* 2014; Berner *et al.* 2015b). The SPBS scheme aims at describing the mechanism of stochastic backscatter of kinetic energy from the near-truncation scales to the larger scales (Shutts 2005; Berner *et al.* 2010, 2012; Romine *et al.* 2014). Both schemes were shown to improve the quality of NWP forecasts, and also to nonlinearly rectify some of the biases in the climate mean and variability in the ECMWF model (Weisheimer and Palmer 2014; Weisheimer *et al.* 2014). More recently, work is being done to test these and other stochastic parameterisation schemes in idealized and more complex climate models for long term integrations (Williams 2012; Ajayamohan *et al.* 2013; Juricke and Jung 2014; Dawson and Palmer 2014).

The merits of stochastic parameterisation are more than just providing estimates of uncertainty in forecast systems. Previous studies have shown that stochastic parameterisation of uncertain model physics can also lead to improvements in the model mean state (Palmer 2001; Berner *et al.* 2012; Weisheimer *et al.* 2014) and climate variability (Dawson and Palmer 2014; Weisheimer *et al.* 2014; Ajayamohan *et al.* 2013; Batte and Doblas-Reyes 2015) through non-linear rectification by small spatial and temporal scales in the stochastic physics impacting large spatial and long temporal climate variability.

Thus the use of stochastic physics in global general circulation models has not only proven beneficial for issuing more reliable probabilistic weather forecasts but also for reducing biases in the mean state and variability on climate timescales. Stochastic parameterisations that change the mean state through non-linear rectification can also affect the response to changes in external forcing (e.g., Seiffert and von Storch 2010). Bridging the gap between the use of stochastic physics in weather and climate simulations is also necessary for a seamless prediction system.

The boundaries between weather prediction and climate prediction models are somewhat artificial (Palmer *et al.* 2008; Hurrell *et al.* 2009; Shapiro *et al.* 2010). Recent advances in prediction on timescales from weather to sub-seasonal to seasonal and decadal by operational weather forecasting centers around the world (Moncrieff *et al.* 2007; Vitart and Robertson 2012) make this artificiality even more evident. Scale interactions of high frequency small scale processes (such as mesoscale and weather scales) with largescale low frequency variability (such as modes of climate variability) both upscale and downscale provide a challenge for accurate weather and climate predictions. For example, there is evidence that natural climate variations, such as El Niño Southern Oscillation (ENSO) on interannual timescales interacts with the MJO on intraseasonal timescales (Hendon *et al.* 2007; Zhang 2005; Subramanian *et al.* 2011; Zhang 2013) and they both can in turn significantly alter the characteristics of extratropical and tropical weather such as cyclones and higher frequency weather events (Vitart and Molteni 2010; Roundy *et al.* 2010; Moon *et al.* 2011; Hoell *et al.* 2014) .

Conversely, small-scale processes have significant upscale effects on large-scale circulation and on the interactions among the components of the global climate system. The key aspect of the seamless prediction challenge for the continuum of weather to climate timescales is the need to characterize the probabilistic forecasts for such a chaotic system.

ECMWF has been at the forefront of dynamical extended range forecasting for more than three decades and is currently leading the global effort in sub seasonal-to-seasonal predictions. There have been many recent advances in the ECMWF model in simulating atmospheric variability, such as improved representation of convectively coupled equatorial Kelvin and Rossby waves, and the Madden-Julian oscillation (MJO) during monthly forecasts (Bechtold *et al.* 2008). The ECMWF Seasonal Forecasting System 4 uses the ECMWF Integrated Forecast System as its atmospheric component, a model used for numerical weather prediction at ECMWF. This atmosperic forecast system also includes the latest development of the SPPT stochastic parametrization scheme.

In this study, we explore the impact of the different scales in the SPPT scheme on the tropical mean and variability in precipitation in the same system. The key tropical modes of variability in our climate system are the ENSO and the MJO, both of which are a coupled ocean-atmosphere phenomena, even though the MJO predominantly manifests as the propagation of atmospheric convection and wind anomalies around the globe. Previous results from studying the impact of stochastic physics in the ECMWF model have shown improvement of the model state with reduced mean state biases and improved representation of the variability on climate timescales (Reyes *et al.* 2009; Weisheimer *et al.* 2014; Batte and Doblas-Reyes 2015; Berner *et al.* 2015a). This motivates the question of how and which aspects of the SPPT scheme in the modeling system impacts the model mean state and variability the most. We explore this question by changing the configuration of the SPPT scheme in the model and studying its impact on the tropical mean precipitation and variability. The results presented in this paper are from the analysis of System 4's seasonal reforecasts with the different configurations of the stochastic physics and then comparing them to a similar set of simulations without stochastic representations of model uncertainty. We find evidence for large scale noise-induced rectification of the ENSO precipitation events and mesoscale and synoptic scale stochastic perturbations to impact the large tropical convective organization in the MJO in these experiments.

The outline of this paper is as follows. In section 2 we describe the seasonal forecasting system, System 4, used for this study and the different experiments evaluated in this study as well as the different metrics and methods used for these evaluations. Results on the changes to the mean precipitation in the Tropics for the different sensitivity experiments are presented in section 3. The impact of the different patterns in the SPPT scheme on the dominant interannual variability in the Tropics, the ENSO, is presented in section 4. The forecast assessment of the dominant tropical mode of intraseasonal variability, the MJO, and the changes to the precipitation in the Tropics during the different phases of the MJO is the subject of Section 5. Section 6 summarizes the main results and presents some conclusions and plans for future work.

2. Model Description and Experiments

ECMWF's seasonal forecasting System 4 (Molteni *et al.* 2011) consists of a coupled ocean-atmosphere system developed for dynamical extended range forecasting and for advancing the capabilities of the previous operational system (System 3). The most significant changes to this system from the previous one are the change in the ocean model component to NEMO (Nucleus for European Modeling of the Ocean), change in the atmospheric component to version CY36R4 of the Integrated Forecasting System (IFS) with improved simulation of tropical intra-seasonal variability and reduced biases in the extratropical regions, higher horizontal and vertical resolution, larger ensemble size in the operational system (51 vs 41 members) and a more sophisticated simulation of model-generated uncertainties. Many of the physical processes in the atmospheric model IFS are parameterized , for example those related to atmospheric convection and clouds, radiative processes in the atmosphere and boundary layer turbulence. In the IFS model, these unresolved diabatic processes are described through a set of deterministic physical parametrization schemes.

The SPPT scheme is one of the stochastic parameterization schemes included in the IFS to represent uncertainty in its physical parameterization tendencies for moisture, heat and momentum. A detailed description of the history of the scheme from its first design (Buizza *et al.* 1999) to its latest implementation is presented in (Palmer *et al.* 2009a). In the SPPT scheme, the sum of the physics tendencies of each of the prognostic variables in the model such as temperature, humidity and momentum is perturbed by a stochastic multiplicative term. The current SPPT scheme has a smooth map of coefficients over space and time and makes use of a spectral pattern generator to define the perturbation coefficients. The scheme uses a univariate distribution for the perturbations that is independent of the variables to be perturbed. The scheme follows equation 1:

$$X_p = (1 + r\mu)X; \tag{1}$$

where, X_p is the perturbed tendency variable, $X = u, v, T, q$ are the parameterized tendencies from the deterministic schemes and $\mu \in [0, 1]$ is the factor used for reducing the perturbation

amplitude close to the surface and in the stratosphere, as perturbations in the near-surface regions have undesirable effects on the ocean, land-surface components such as numerical instabilities, while perturbations in the stratosphere are not desired due to the negligible uncertainty in the clear sky radiation tendencies in the stratosphere.

The perturbation patterns of r have three defined spatio-temporal decorrelation scales and follow an autoregressive model of order 1 (AR1). The three scales of perturbations have characteristic lengths of : (i) 500 km and 6 h decorrelation representing the uncertainty in mesoscale processes, (ii) 1000 km and 3 days representing the synoptic scale uncertainties in physical tendencies and (iii) 2000 km and 30 days decorrelation representing the uncertainty in the large scale impact of subgrid scale physics tendencies. A unique and interesting feature of this stochastic scheme is that the three scales can be combined linearly as two or more independent patterns to account for model errors at different temporal and spatial scales. The variance of each of these stochastic terms are predetermined and represent the magnitude of the uncertainty in each of these scales. The shortest scale is defined to have the largest amplitude of perturbations signifying that the largest uncertainty lies in the mesoscale physical tendencies. The second and third scales have a lower and the lowest variance correspondingly, signifying that these scales which are partially and fully resolved by the model grid scale dynamics have lower uncertainty.

The amplitude of the variance for each of these patterns has been motivated by results from coarse-graining studies with cloud resolving models (Palmer *et al.* 2009a; Shutts and Palmer 2007). For instance, Shutts and Palmer (2007) showed that the standard deviation of the temperature tendency in a high-resolution cloud resolving simulation is linearly related to the mean temperature tendency and hence, lends support to a multiplicative noise scheme like SPPT for modeling uncertainty in convective parameterizations. Some theories such as Craig and Cohen (2006) argue that temperature tendency errors in convective parameterization behave like a Poisson process, where the variance of the tendency is linearly proportional to the mean temperature tendency. This is also shown in numerical results from a more recent coarse-graining study by Shutts and Pallarès (2014). Another recent study by Watson *et al.* (2015) shows that IFS with the multiplicative-noise SPPT scheme reproduces the observed ratio of the standard deviation to the mean of precipitation as a function of both relative humidity and vertical velocity in the Tropics. Hence, these recent findings imply that though the ECMWF stochastic perturbed parameterization tendency scheme reproduced some of the observed features of convection, it can be improved further, and its benefits in improving the model spread and skill at short and seasonal timescales can be further enhanced.

Table 1. Variance of perturbations applied for the temporal and spatial decorrelation scales in the noSPPT, SPPT, SPPT1d, SPPT2x and SPPT3x experiments. Each pattern is linearly combined according to the σ coefficient

Experiment name	Scale 1 (500 km, 6h)	Scale 2 (1000 km, 3d)	Scale 3 (2000 km, 30d)
noSPPT	0	0	0
SPPT	0.52	0.18	0.06
SPPT1d	0.70	0.18	0.06
SPPT2x	0.52	0	0.06
SPPT3x	0.52	0.18	0

The parameter settings for SPPT used in System 4 are exactly the same as those used in ECMWFs operational medium-range weather forecasting system. In this study, we use a similar setting to those used for ECMWF System 4 in our control experiment (SPPT). Recent results from an experiment similar to the SPPT presented in (Weisheimer *et al.* 2014) show the benefits of representing model errors in rectifying the mean biases and in improving the spread-skill ratio at monthly-to-seasonal timescales. We further examine the impact of SPPT on tropical precipitation mean and variability biases in a similar setup with three other sensitivity experiments. One of the experiments, SPPT1d hereafter, has the standard deviation of the first scale amplified by ≈ 1.33 times its default value to study the impact of assuming a higher error variance for the mesoscale compared to the default settings. The next two experiments, called SPPT2x and SPPT3x, were designed with one of the two larger scales deactivated (the second and third scale respectively). These were done as a denial experiments to understand how these two scales impact the mean and variability in tropical precipitation, as these three SPPT scales can be combined linearly by design. Table 1 shows the details of the standard deviation parameter used for each of the three scales in the five different experiments.

By design, the regions with correlated values of r are going to have larger areas in the SPPT2x case than the SPPT3x case, and the temporal evolution of r will be slower in SPPT2x compared to SPPT3x, where only the first and second scales are active. The SPPT1d case is likely to have a faster temporal decorrelation than SPPT2x or SPPT3x, as the first scale (high frequency) stochastic term has increased variability. Leaving out the synoptic scale or large scale stochastic terms in SPPT2x and SPPT3x experiments respectively implies that the tendencies are affected by the first scale of SPPT in both these cases and we can discern how the lack of the large scales vs synoptic scale perturbations will systematically amplify or reduce the tendencies and hence impact the mean and variability in the tropical climate. Similarly, SPPT1d experiment compared to the SPPT experiment will help understand the impact of the first scale (high frequecy stochastic term) on the tropical precipitation statistics.

The atmospheric model IFS is run in horizontal spectral resolution of T255 (approximate grid size of 80 km) and 91 vertical levels up to 0.01 hPa for all the experiments. The ocean model used in System 4 is the NEMO v3.0, a state-of-the-art three-dimensional general circulation model. The ocean model has 42 levels in the vertical and the horizontal resolution is approximately 110 km (1°) with equatorial refinement. The atmosphere and the ocean model components are coupled at 3 h intervals using the OASIS3 coupler (Molteni *et al.* 2011).

An extensive set of re-forecast experiments were run for the past two decades for all five experiments with 15 ensemble members in each experiment. We further analyse the difference in the mean state and variability amongst these experiments to understand the impact of the different stochastic patterns. The experiments analysed here were re-forecasts for boreal winter months initialized on November 1^{st} of each year from 1991-to-2009. The different initial conditions for the ensemble members were generated from a combination of ocean and atmospheric re-analyses and perturbations to the wind and SST fields over the ocean (Molteni *et al.* 2011). The atmospheric model has been initialized using the ERA-Interim reanalysis (Dee *et al.* 2011) with ECMWF's operational singular vector perturbations for the atmospheric fields. The ocean fields are initialized from the ORA-S4 NEMOVAR five-member ensemble reanalysis (Balmaseda *et al.* 2013). During the model integration, each ensemble member samples a different realization of the uncertainty in the sub-grid scale physics tendencies in the atmosphere using the SPPT scheme.

Here, we study the impact of the different SPPT stochastic perturbation scales on mean, inter-annual and intraseasonal variability of the tropical precipitation field. The dominant inter-annual variability in the Tropics is the El Niño Southern Oscillation (ENSO) and the dominant intraseasonal variability in the Tropics is the Madden-Julian Oscillation (MJO).

We identify strong El Niño (La Niña) events by computing the Niño 3.4 index and identifying events with three month mean values of the index above (below) the threshold of +1.0°C (-1.0°C). For the MJO forecast skill in the different experiments, we compute the bivariate correlation (COR) and Root Mean Square Error (RMSE) between the observed and forecast Realtime Multivariate MJO (RMM) indices using the method as described in Lin *et al.* (2008). We also compute a probabilistic score, the continuous ranked probability skill score (CRPSS), to measure the forecast skill in the different experiments. The bivariate correlation is defined as:

$$COR(\tau) = \frac{\sum_{t=1}^{N}[pc_1^o(t)pc_1^m(t,\tau) + pc_2^o(t)pc_2^m(t,\tau)]}{\sqrt{\sum_{t=1}^{N}[pc_1^o(t)^2 + pc_2^o(t)^2]}\sqrt{\sum_{t=1}^{N}[pc_1^m(t)^2 + pc_2^m(t)^2]}}, \quad (2)$$

where $pc_1^o(t)$ and $pc_2^o(t)$ are the first two principal components of the RMM analysis for the verification dataset at time t, $pc_1^m(t,\tau)$ and $pc_2^m(t,\tau)$ are the first two principal components of the RMM analysis of the model forecast fields at time t with a lead time of τ days and N is the total number of forecast events considered. The RMSE is defined as:

$$RMSE(\tau) = \sqrt{\frac{1}{N}\sum_{t=1}^{N}[(pc_1^o(t) - pc_1^m(t,\tau))^2 + (pc_2^o(t) - pc_2^m(t,\tau))^2]}, \quad (3)$$

The CRPSS is a skill score based on a measure of the integrated squared difference between the cumulative distribution function of the forecasts and the corresponding cumulative distribution function of the observations .

The characteristics of these metrics and examples of their use to evaluate global model forecasts are discussed in Gottschalck *et al.* (2010). First, we present the results from the analysis of the difference in the mean precipitation for the different experiments in the next section.

3. Stochastic perturbations and tropical mean precipitation

Stochastic parameterizations can theoretically influence the mean state of climate models and hence, if rectified in the right direction, they can reduce the mean bias of the model against observations. In other words, stochastic perturbations can occasionally shift the system away from its preferred modes of variability and hence, statistically, change the mean state as well as the climate variability of the system. The first aspect of the impact of the different patterns in the SPPT scheme we study is the change in the mean precipitation of the model. We focus our study on the tropical region (15 °N to 15 °S), since this is the region dominated by deep convection and hence, is most affected by the stochastic perturbations to the physical tendencies as shown in Weisheimer *et al.* (2014). We examine these impacts by evaluating the error in each of the SPPT experiments relative to the noSPPT experiment.

Figure 1 shows the difference in daily mean precipitation of each individual SPPT experiment with that of the experiment with no stochastic perturbations. The stochastic perturbations in all four of the sensitivity experiments show an overall reduction of the positive precipitation bias in System 4. Figure 2a shows the probability density function (PDF) of precipitation over a small region in the west Pacific for the runs with (red line) and without (black line) stochastic physics. The difference in the two histograms are plotted as the two bottom subpanels in Figure 2a. These two sub-panels show the increase in occurrence of low precipitation days and in the extreme high precipitation days accompanied by a reduction in the precipitation mode.

The stochastic perturbations of SPPT on the physics tendencies in the ECMWF model are perturbations on the convective tendencies and hence precipitation via the conservation of enthalpy. We explore the expected change in the precipitation PDF given a stochastic noise term using a simple model for time varying precipitation (associated with convection in the model). The PDF of precipitation is typically modeled as a Gamma distribution or as a lognormal distribution (Cho *et al.* 2004) for station data or satellite observations. Here, we model the precipitation as a random variable with an idealized Gamma distribution as shown in black in Figure 2b. The perturbations to the the precipitation time series are non-zero above a threshold in the simple model (similar to a convective trigger function in atmospheric models). The noise term is modeled as a conditionally Gaussian (or Gaussian-Jump) process. The threshold is shown by the blue line in the top panel of Figure 2b. The difference in the newly generated PDF of precipitation and the PDF of the original precipitation time-series is shown in the bottom two panels with the grey line. This resembles the change in PDF for the precipitation when stochastic physics is switched on. Hence, in this simple model, the stochastic physics shifts the mean of the PDF towards a drier state. Though this simplified model of stochastic perturbations to precipitation may not accurately depict all the effects of SPPT in IFS, it still captures the essence of the change in precipitation PDFs where convection is active. This is also consistent with enhanced perturbations (in SPPT1d) decreasing the mean bias even further in the ITCZ region. The reduction in convection and precipitation over the warm pool - Maritime continent region will further reduce the upward Mass flux and hence weaken the Walker circulation over the Tropical Pacific region. This will have additional circulation driven changes to precipitation and convection, which are nonlinear effects to be disentangled with further analysis. We discuss this result in more detail in Section 6.

We further note that the position of the Inter-Tropical Convergence Zone (ITCZ) is altered by the stochastic schemes by restricting the precipitation in the ITCZ band to a narrower region north of the equator with most of the reduction in mean precipitation between 5 °N and 10 °N and a slight increase in mean precipitation between the equator and 5 °N for all the experiments (Fig. 1). The experiment with the amplified mesoscale stochastic perturbations (SPPT1d) shows further reduction in the mean precipitation bias though the spatial

Table 2. Reliability and Brier Skill Scores for precipitation anomalies below the lower tercile in the noSPPT, SPPT, SPPT1d, SPPT2x and SPPT3x experiments for DJF from 1991-2010. 95% confidence intervals are in brackets.

Experiment name	Brier Skill Score	Reliability Skill Score
noSPPT	0.093 (0.042, 0.145)	0.961 (0.950, 0.968)
SPPT	0.1 (0.057, 0.147)	0.966 (0.955, 0.973)
SPPT1d	0.115 (0.067, 0.160)	0.974 (0.961, 0.980)
SPPT2x	0.106 (0.057, 0.151)	0.969 (0.959, 0.975)
SPPT3x	0.097 (0.045, 0.148)	0.965 (0.952, 0.974)

Table 3. Reliability and Brier Skill Scores for precipitation anomalies above the upper tercile in the noSPPT, SPPT, SPPT1d, SPPT2x and SPPT3x experiments for DJF from 1991-2010. 95% confidence intervals are in brackets.

Experiment name	Brier Skill Score	Reliability Skill Score
noSPPT	0.080 (0.038, 0.120)	0.960 (0.947, 0.970)
SPPT	0.107 (0.065, 0.149)	0.975 (0.965, 0.981)
SPPT1d	0.108 (0.064, 0.146)	0.975 (0.965, 0.982)
SPPT2x	0.109 (0.064, 0.150)	0.975 (0.965, 0.982)
SPPT3x	0.095 (0.051, 0.137)	0.971 (0.960, 0.980)

pattern in the difference is similar, while the SPPT2x and SPPT3x experiments show very little difference as compared to the default experiment SPPT. The position of the ITCZ is determined by many factors. An emerging framework in recent idealized modeling studies (Schneider *et al.* 2014; Frierson *et al.* 2013) links the ITCZ position to the atmospheric energy balance between the two hemispheres. Further studies on how stochastic perturbations impact global energy transport in longterm climate simulations with stochastic physics is encouraged. Some of the first longterm climate simulations with SPPT and other stochastic physics are underway currently (Berner *et al.* 2015a).

Figure 3 shows the ensemble standard deviation for the daily mean precipitation for each experiment. The spread in the mean precipitation is highest in the Western Pacific and Central Pacific region between 5 °N and 5 °S. It is also enhanced in the Southern side of Eastern Equatorial Pacific where there is very little mean precipitation and very little change in mean precipitation for these experiments as seen in Figure 1. Increased amplitude of the mesoscale stochastic perturbations tend to increase the spread marginally, while keeping the pattern of change in spread the same (as seen in Fig. 3b). Switching off the second scale in the SPPT scheme (SPPT2x) has very little impact on the spread change, while switching off the third scale (SPPT3x) seems to shrink the region of increased spread in the West/Central Pacific for SPPT experiment to be mostly in the Central Pacific.

We further list a probabilistic skill score, the Brier skill score (BSS), for tropical precipitation anomalies in these experiments in Table 2 and Table 3. Table 2 shows the Brier skill score for the precipitation anomalies below the lower tercile in the different experiments. The SPPT1d experiment has the highest BSS followed by SPPT2x and SPPT experiments. The noSPPT model forecasts have the least BSS. Decomposition of the BSS shows that the SPPT1d case has higher reliability and resolution(not shown). For the precipitation anomalies exceeding the upper tercile (Table 3), the SPPT, SPPT1d and SPPT2x experiments have a similar BSS and reliability as well as resolution skill scores.

4. Stochastic perturbations and ENSO

Given that the stochastic perturbations to the physical tendencies from the SPPT scheme has a positive impact on the tropical mean precipitation especially over the Maritime continent, tropical Western Pacific and the ITCZ region by reducing the excess precipitation bias, we would expect it to have an impact on the strongest interannual variability in the region, the ENSO, too. In this section, we analyse how the different configurations of the stochastic perturbations affect the composite precipitation in the Tropics during El Niño and La Niña events.

Figure 4 shows the composite mean precipitation in the tropical region for five different El Niño events during DJF for the four experiments. We see a similar change in pattern of precipitation as seen in the total mean precipitation for 20 years, except that the mean increase in precipitation (region with positive precipitation anomalies compared to noSPPT) has shifted towards the central Pacific region. The precipitation in the Central Pacific is amplified due to stochastic perturbations and the precipitation in the ITCZ is reduced. This pattern is further amplified when the mesoscale stochastic perturbations are amplified (Fig 4b). Even though the precipitation in the central and eastern Pacific is enhanced in an anomalous sense the total precipitation and convection amplitude in El Niño conditions is weaker than the net convection in the West Pacific during an ENSO neutral phase. Since the stochastic perturbations are multiplicative, they tend to amplify or dampen large signals in convection but do not have much impact on weaker convective events. The first scale of perturbations in SPPT1d

experiment tends to amplify the change in precipitation, similar to the change in 20-year mean precipitation (Fig. 4b). Deactivating the second scale of perturbations in experiment SPPT2x tends to weaken the impact of the stochastic scheme in general, while the lack of the largescale perturbations in SPPT3x does not seem to impact the change in mean precipitation significantly (Fig. 4 c,d) during El Niño events.

The change in precipitation between the different SPPT experiments and noSPPT experiment during La Niña events is shown in Figure 5. Most of the change in precipitation during La Niña events is confined to the West Pacific and Maritime continent region unlike during El Niño events. The pattern is largely similar to the change patterns for the 20-year mean precipitation as in Figure 1, except in the central Pacific region where there is no difference. There is reduced precipitation between 5 °N and 10 °N and enhanced precipitation between 5 °N and the equator and also along the South Pacific Convergence Zone. This is also due to the convection over the West Pacific and Maritime continent being anomalously amplified during La Niña events. Hence, the stochastic perturbations can impact these regions more, due to the increase in physical tendencies of temperature and moisture during La Niña events. The central and East Pacific regions do not see much change in precipitation due to stochastic physics as the convection is suppressed in these regions.

We further investigate the change in ensemble standard deviation for the DJF mean precipitation in the different experiments. Figure 6 shows the composite change in standard deviation for El Niño events. The ensemble spread for the SPPT experiment increases in the central and east Pacific regions, with no significant increase in the west Pacific region. This is expected as the net convection in the Western Pacific region has reduced and hence the impact of a multiplicative stochastic noise will be weak here. Amplifying the first scale in the SPPT scheme (SPPT1d experiment) amplifies the standard deviation in the same spatial pattern over the Central and East Pacific regions as in the SPPT experiment. Hence, the mesoscale perturbations to the physics tendencies have an upscale effect to impact the ensemble spread in seasonal mean precipitation for the El Niño and La Niña events. During La Niña events, the ensemble standard deviation amplifies over the West Pacific, and Maritime continent regions with no significant change in ensemble spread in the central and East Pacific, because the convection in the West Pacific region is anomalously amplified while the convection over the central and east equatorial Pacific regions are anomalously damped during La Niña events. Hence, the stochastic perturbations in the ensemble members can be expected to increase the variance where the convection is seated (Fig. 7). Both the SPPT1d and SPPT2x experiments do not show any significant change in ensemble spread compared to the SPPT case, while switching off the largescale perturbations, as in SPPT3x experiment, seems to considerably decrease the spread in the West Pacific region compared to the SPPT case. It was noted that the three scale SPPT scheme excites a divergence in the ENSO SSTs in System 4, and hence leads to a larger spread in the ENSO forecasts as compared to the single scale SPPT scheme in System 3 (Molteni *et al.* 2011). Weisheimer *et al.* (2014) also showed that the SPPT scheme in System 4 leads to reduced Root Mean Square Error (RMSE) and increased ensemble spread for ENSO forecasts, leading to a more reliable ensemble forecasting system as compared to having to model uncertainty representation. From our analysis, we see that the first and the third scales of stochastic perturbations play a more important role in modulating the precipitation and convection behavior during El Niño and La Niña states. Next we describe the changes to forecast skill of the MJO and variability in tropical precipitation at intraseasonal timescales due to stochastic physics.

5. Stochastic perturbations and the MJO

We study the Madden-Julian Oscillation in the 20 year (1991-2009) seasonal forecasts, both as a function of phase and as a forecast skill dependency on the stochastic perturbations. Figure 8a shows the bivariate correlation coefficient of the first two Principal Components of the multivariate EOF analysis for the MJO over the 20 years of winter time forecasts. The bivariate correlation coefficient is computed as defined in Gottschalck *et al.* (2010) and presented in Section 2. The skill in MJO forecasts are very comparable for the first week in all five experiments with the reduction in correlation of 0.1. In week two, the deterministic ensemble has the least skill and the forecasts made in the SPPT1d case has higher correlation and increased skill compared to the other experiments. As we move into week three and four, the

skill of the experiments SPPT2x and SPPT3x drop below the skill of SPPT1d and the noSPPT ensemble. This implies that switching off the second and third scale in the SPPT scheme adversely impacts the MJO forecast skill in the model for periods beyond 2 weeks. The decorrelation timescales in the second and third scale of SPPT are 3 days and 30 days and hence, it is reasonable to assume that they impact atmospheric variability on these timescales directly. Predictability at subseasonal-to-seasonal timescales is a key challenge for the forecasting community currently (Vitart 2014) and having a reliable forecasting system for the MJO is one of the key aspects of this challenge.

Many previous studies (Majda and Stechmann 2009; Frenkel *et al.* 2012; Kondrashov *et al.* 2013; Chen and Majda 2014) have shown the importance of high frequency convective wave activity in the maintenance and propagation of the MJO and the use of stochastic parameterizations in MJO prediction skill. Tropical convection has a rich multiscale dynamics with the interaction of the different physical aspects such as radiation, convection and boundary layer dynamics. The largescale waves in the Tropics cannot be approximated as a linear combination of the small scale waves they envelope. Recent results (summarized in Zhang (2013); Majda and Stechmann (2012)) show that the MJO is an envelope of smaller scale convective systems, including mesoscale convective systems (MCS), tropical cyclones, and synoptic scale waves with interactions between the synoptic scale waves and their larger scale environment playing a key role in the mechanisms to maintain the MJO. Hence, representing these mesoscale and synoptic scale variability more accurately would have an impact on the MJO in a model. We see that all three scales in the SPPT scheme (mesoscale, synoptic scale and largescale) have an impact on the MJO at different forecast lead times.

Figure 8b shows the Root Mean Square Error (RMSE, continuous lines) and the ensemble spread (dashed lines) for the same 20 years of winter time forecasts as mentioned above. The RMSE for the first two principal components of the multivariate EOF analysis is also computed as defined in Gottschalck *et al.* (2010). The RMSE skill score for each experiment shows a similar relative skill as does the bivariate correlation metric. All experiments in week one have a similar skill, except that the noSPPT ensemble has a lower spread than the other experiments and hence is a less reliable ensemble. Yet, all experiments have a lower ensemble spread than the RMSE at all lead times and hence, are underdispersive and unreliable ensemble prediction systems for the MJO. The deterministic forecasts (noSPPT) have the least ensemble spread and the highest error in the week 2. This implies that the deterministic ensemble is the least reliable ensemble for forecasting the MJO in week 2. The SPPT1d experiment has the least RMSE for all weeks except week 3, while it also has the highest spread, implying that the ensemble is more reliable than the other experiments. The experiments SPPT2x and SPPT3x have the highest errors in week 3-4, though their spread is still higher than that of the deterministic case and is comparable to the SPPT1d and SPPT cases. This implies that the second and third scales in the SPPT scheme impacts tropical intraseasonal forecasts at time ranges of week 3-4 which is a critical timerange for subseasonal-to-seasonal prediction (Vitart and Robertson 2012) to bridge the gap between weather and seasonal prediction. Synoptic scale and largescale errors, when not represented by the stochastic physics can have nonlinear detrimental impacts on longer term variability and predictability, such as on the subseasonal timescale.

Figure 8c,d displays the evolution of the CRPSS of the RMM1 and RMM2 respectively over the first six weeks. Figure 8c shows that there is a significant drop in probabilistic prediction skill in week 4 for all the experiments. While all the experiments have equivalent skill in the first week of the forecasts, the noSPPT experiment has the least skill in week 2 and 3. Beyond week 3, all experiments have similar skill in forecasting both the RMM1 and RMM2 within confidence intervals. Overall the SPPT1d experiments has higher skill through the whole period, although it is within the forecast uncertainty of other experiments (SPPT2x and SPPT3x).

Next we look at how the composite precipitation patterns change in different phases of the MJO for the different experiments. Figure 9 shows a composite map of biases in total daily mean precipitation anomalies for the noSPPT case compared to observed precipitation anomalies in the Global Precipitation Climatology Project (GPCP Adler *et al.* 2003), where the blue shades indicate regions with positive precipitation anomalies in the GPCP compared to noSPPT and shades of red indicate

regions of suppressed convection and precipitation in GPCP compared to noSPPT. Starting from phase 1 in the top panel, we see a positive anomaly indicating increased precipitation and convection in the noSPPT experiment compared to GPCP in largescale convective region of the MJO propagate from the West Indian Ocean region into the West Pacific and central Pacific over the eight phases. The region of suppressed convection east of the convective center of the MJO also shows reduced suppression or increased precipitation in GPCP compared to noSPPT. This signal then propagates along with precipitating region through the eight phases.

We next show how these precipitation anomalies change for the different sensitivity experiments of SPPT. Figure 10 shows the composite maps of difference in daily mean precipitation anomaly between the SPPT and noSPPT experiments during the eight phases of the MJO. In the first two phases, when the MJO convection is centered in the Western and Central Indian Ocean, with the suppressed phase over the Maritime Continent-West Pacific region, the SPPT scheme tends to suppress the precipitation and convection over the West Pacific even further. Kim *et al.* (2013); Ling *et al.* (2013) show that for a propagating MJO event, the suppression over the Maritime continent and West Pacific region is critical compared to non-propagating largescale convective events over the Indian Ocean. Hence, this implies that with enhanced suppression over the West Pacific region for the SPPT experiment, it would tend to propagate these MJO events more actively. The SPPT experiment also has reduced precipitation over the Indian Ocean region in these phases and hence, is more consistent with observations. This then indicates that the noSPPT experiment bias is reduced, albeit only by 50% or less.Weisheimer *et al.* (2014) showed from statistical analysis that there were more MJO events when stochastic physics was active in the model. In our results, the first two phases of the MJO show enhanced suppression in the West Pacific with stochastic perturbations, which is consistent with increased MJO events for stochastically forced seasonal forecasts (Weisheimer *et al.* 2014) and is supported by the results of Kim *et al.* (2013). In the other phases, when the MJO is propagating, the maps show that the MJO in the SPPT case has increased precipitation in the suppressed phases and reduced precipitation in the active phases of the MJO in Maritime Continent and West Pacific regions. These anomalous differences propagate along with the MJO and are consistent with reducing the noSPPT bias compared to GPCP observed anomalies.

Studying the other SPPT experiments, Figure 11 shows the composite maps of difference in daily mean precipitation anomaly between the SPPT1d and noSPPT experiments during the eight phases of the MJO. The change in precipitation anomaly for the SPPT1d experiment also shows a similar pattern as the SPPT case. The biases in the SPPT2x and SPPT3x experiment compared to noSPPT are similar to the SPPT1d case (not shown). The SPPT3x experiment shows that in phases 4 to 8, the precipitation in the suppressed phase of the MJO is enhanced compared to the other three SPPT sensitivity experiments indicating that the third (long-term) stochastic perturbation pattern has an impact on the subseasonal scale, which when removed deteriorates the model MJO fidelity . Thus overall, all three SPPT scales of perturbations have a nonnegligible positive impact on the MJO composite precipitation and also on the forecast skill of the MJO.

6. Discussion and Conclusions

The impact of different configurations of the stochastic parameterization scheme in the atmospheric model of ECMWF's coupled seasonal forecast System 4 was assessed. We used re-forecasts from 1^{st} November start dates over a 20 year period (1991-2009) for this study and examined how the different scales of perturbations in the SPPT scheme affected the mean state and variability of the precipitation. The SPPT scheme used in this study is also used in ECMWF's medium-range ensemble weather forecasts to perturb the total tendencies of all diabatic physical processes parameterized in the model. Results of sensitivity experiments of SPPT scales in terms of changes in systematic errors, changes in bias in interannual and intraseasonal variability and also spread-skill ratio and correlation for MJO forecasts were shown over the Tropical region.

It was found that forecast system with no stochastic perturbations has excessive precipitation bias in the Maritime Continent, West Pacific and ITCZ regions over the Tropics. The stochastic perturbations to the tendencies reduce this excessive convection bias in these areas, leading to an improved mean

state of precipitation in the model. We show with a simple stochastic model on an idealized time series that a jump-diffusion process can reduce the mean of the distribution due to its asymmetric forcing. This reduction in convection over the Maritime continent also leads to reduced upward mass flux in the region weakening the Walker circulation. This has consequences on the Walker circulation and the meridional circulation. The position of the ITCZ was also shifted southward in the northern hemisphere with stochastic perturbations. Amplifying the first scale of perturbations tends to reduce the bias in precipitation even further over the ITCZ region. Yet, deactivating the second or the third scale in SPPT did not seem to impact the reduction in mean bias of precipitation significantly. This implies that the small/fast scale perturbations in SPPT tend to impact the mean precipitation the most. In terms of ensemble spread in the mean precipitation, switching off the third scale reduced the area of enhanced ensemble spread compared to the SPPT experiment.

Along with systematic bias reduction in the tropical precipitation, it was found that the stochastic perturbations tend to increase precipitation in the Central and East Pacific region during El Niño events and increase precipitation in the West Pacific region during La Niña events. Such change in convective activity in phase with the ENSO anomalous convection could lead to enhanced SST-atmospheric winds-convection feedback (Bjerknes 1969) and further impact the ENSO event's evolution. Analysis of the sensitivity experiments showed that deactivating the second scale in the SPPT scheme tends to weaken the bias reduction in precipitation. Although the third scale (largescale) perturbations do not have much impact on the ENSO composite mean precipitation, they do have an impact on the ensemble spread for an ENSO event and switching them off decreases the ensemble spread significantly. The ensemble standard deviation during ENSO events is correspondingly increased for all experiments in regions centered around the convective centers of the ENSO events.

Previous studies (such as Jin *et al.* (2007); Zavala-Garay *et al.* (2008); Perez *et al.* (2005)) show that probability of an El Niño event is modified by high frequency convective wave activity in the Tropics and that, in turn, the convective wave activities are regulated by ENSO activity. They further show that simple additive stochastic forcing would not capture such nonlinear scale interactions sufficiently and having multiplicative noise terms in the system equations helps reproduce the observations better. The results presented here are consistent with previous studies performed with the ECMWF seasonal forecast system (Reyes *et al.* 2009; Weisheimer *et al.* 2014, 2011).

Another significant mode of climate variability in the Tropics is the MJO and it has been a long standing challenge to model and predict the MJO accurately (Zhang *et al.* 2013). The ECMWF forecast system, being one of the best models in the world currently for MJO forecasts (Klingaman *et al.* 2015), still underestimates the frequency and amplitude of the daily MJO events as well as the forecast skill-spread ratio. Here, we have shown that amongst the different configurations of the SPPT scheme, amplifying the first scale (mesoscale) perturbation in SPPT improves the MJO skill scores while, deactivating the second and third scales adversely affect the MJO skill score on lead times beyond two weeks.

Composite maps of precipitation during the different phases of the MJO show that the stochastic perturbations tend to enhance the suppressed phase of the MJO in the first two phases, as the MJO initiates and begins to propagate across the Indian Ocean. Once the MJO is active, the stochastic perturbations tend to dampen the precipitation anomalies during active phases and enhance the precipitation anomaly in the suppressed phases.

We have further analysed other re-forecast runs in a similar setup and find similar results for the impact of SPPT scheme in the ECMWF IFS model. Yet, one drawback of this study is that the re-forecast period of 20 years and 15 ensemble members used in this study may not be sufficient to obtain statistically significant results, especially for the interannual variability analysis. In summary, based on the the conclusions from the different SPPT1d, SPPT2x and SPPT3x experiments discussed here for the precipitation variability over the Tropical Pacific region, the rectification of the model mean state and improvement in the model variability is certainly obtained by the stochastic perturbations. We separate the impacts of the small scale from the large scale stochastic perturbation patterns, yet show that all three scales are important for error reduction in the mean and variability of the Tropical climate.

Acknowledgements

AW would like to acknowledge funding from the EU-FP7 project SPECS (grant agreement 308378). TP and AS thank the ERC grant 291406. AS also thanks the NOAA grant NA14OAR4310276. The GPCP combined precipitation data were developed and computed by the NASA/Goddard Space Flight Center's Laboratory for Atmospheres as a contribution to the GEWEX Global Precipitation Climatology Project.

References

Adler RF, Huffman GJ, Chang A, Ferraro R, Xie PP, Janowiak J, Rudolf B, Schneider U, Curtis S, Bolvin D, *et al.* 2003. The version-2 global precipitation climatology project (gpcp) monthly precipitation analysis (1979-present). *Journal of Hydrometeorology* **4**(6): 1147–1167.

Ajayamohan RS, Khouider B, Majda AJ. 2013. Realistic initiation and dynamics of the Madden-Julian Oscillation in a coarse resolution aquaplanet GCM. *Geophysical Research Letters* **40**(23): 6252–6257.

Balmaseda MA, Mogensen K, Weaver AT. 2013. Evaluation of the ECMWF ocean reanalysis system ORAS4. *Quarterly Journal of the Royal Meteorological Society* **139**(674): 1132–1161.

Batte L, Doblas-Reyes FJ. 2015. Stochastic atmospheric perturbations in the EC-Earth3 global coupled model: impact of SPPT on seasonal forecast quality. *Climate Dynamics* **45**(11-12): 3419–3439.

Bauer P, Thorpe A, Brunet G. 2015. The quiet revolution of numerical weather prediction. *Nature* **525**(7567): 47–55.

Bechtold P, Köhler M, Jung T, Doblas-Reyes F, Leutbecher M, Rodwell MJ, Vitart F, Balsamo G. 2008. Advances in simulating atmospheric variability with the ECMWF model: From synoptic to decadal time-scales. *Quarterly Journal of the Royal Meteorological Society* **134**: 1337–1351.

Berner J, Achatz U, Batte L, De La Camara A, Crommelin D, Christensen H, Colangeli M, Dolaptchiev S, Franzke CLE, Friederichs P, Imkeller P, Jarvinen H, Juricke S, Kitsios V, Lott F, Lucarini V, Mahajan S, Palmer TN, Penland C, von Storch JS, Sakradzija M, Weniger M, Weisheimer A, Williams PD, Yano JI. 2015a. Stochastic Parameterization: Towards a new view of Weather and Climate Models. *arXiv.org* .

Berner J, Jung T, Palmer TN. 2012. Systematic Model Error: The Impact of Increased Horizontal Resolution versus Improved Stochastic and Deterministic Parameterizations. *Journal of Climate* **25**(14): 4946–4962.

Berner J, Shutts GJ, Leutbecher M, Palmer TN. 2010. A Spectral Stochastic Kinetic Energy Backscatter Scheme and Its Impact on Flow-Dependent Predictability in the ECMWF Ensemble Prediction System. *Journal of the Atmospheric Sciences* **66**(3): 603–626.

Berner J, Smith KR, Ha SY, Hacker JP, Snyder C. 2015b. Increasing the skill of probabilistic forecasts: Model-error representations versus calibration and debiasing. *Mon. Wea. Rev* **143**: 1295–1320.

Bjerknes J. 1969. Atmospheric teleconnections from the equatorial pacific. *Monthly Weather Review* **97**(3): 163–172.

Bony S, Stevens B, Frierson DMW, Jakob C, Kageyama M, Pincus R, SHEPHERD TG, Sherwood SC, Siebesma AP, Sobel AH, Watanabe M, Webb MJ. 2015. Clouds, circulation and climate sensitivity. *Nature Publishing Group* **8**(4): 261–268.

Brunet G, Shapiro M, Hoskins B, Moncrieff M, Dole R, Kiladis GN, Kirtman B, Lorenc A, Mills B, Morss R, Polavarapu S, Rogers D, Schaake J, Shukla J. 2010. Collaboration of the Weather and Climate Communities to Advance Subseasonal-to-Seasonal Prediction. *Bulletin of American Meteorological Society* **91**(10): 1397–1406.

Buizza R, Milleer M, Palmer TN. 1999. Stochastic representation of model uncertainties in the ECMWF ensemble prediction system. *Quarterly Journal of the Royal Meteorological Society* **125**(560): 2887–2908.

Chen N, Majda AJ. 2014. Predicting the Real-time Multivariate Madden-Julian Oscillation Index through a Low-Order Nonlinear Stochastic Model. *Monthly Weather Review* **143**: 2148–2169.

Cho HK, Bowman KP, North GR. 2004. A comparison of gamma and lognormal distributions for characterizing satellite rain rates from the tropical rainfall measuring mission. *Journal of Applied Meteorology* **43**(11): 1586–1597.

Craig GC, Cohen BG. 2006. Fluctuations in an equilibrium convective ensemble. Part I: Theoretical formulation. *Journal of the Atmospheric Sciences* **63**: 1996–2004.

Dawson A, Palmer TN. 2014. Simulating weather regimes: impact of model resolution and stochastic parameterization. *Climate Dynamics* : 1–17.

Dee DP, Uppala SM, Simmons AJ, Berrisford P, Poli P, Kobayashi S, Andrae U, Balmaseda MA, Balsamo G, Bauer P, Bechtold P, Beljaars ACM, van de Berg L, Bidlot J, Bormann N, Delsol C, Dragani R, Fuentes M, Geer AJ, Haimberger L, Healy SB, Hersbach H, Holm EV, Isaksen L, Kallberg P, Koehler M, Matricardi M, McNally AP, Monge-Sanz BM, Morcrette JJ, Park BK, Peubey C, de Rosnay P, Tavolato C, Thepaut JN, Vitart F. 2011. The ERA-Interim reanalysis: configuration and performance of the data assimilation system. *Quarterly Journal of the Royal Meteorological Society* **137**(656): 553–597.

Durran DR, Gingrich M. 2014. Atmospheric Predictability: Why Butterflies Are Not of Practical Importance. *Journal of Atmospheric Sciences* **71**(7): 2476–2488.

Frenkel Y, Majda AJ, Khouider B. 2012. Using the Stochastic Multicloud Model to Improve Tropical Convective Parameterization: A Paradigm Example. *Journal of the Atmospheric Sciences* **69**(3): 1080–1105.

Frierson DMW, Hwang YT, Fučkar NS, Seager R, Kang SM, Donohoe A, Maroon EA, Liu X, Battisti DS. 2013. Contribution of ocean overturning circulation to tropical rainfall peak in the Northern Hemisphere. *Nature Geoscience* **6**(11): 940–944.

Gottschalck J, Wheeler M, Weickmann K, Vitart F, Savage N, Lin H, Hendon HH, Waliser DE, Sperber K, Prestrelo C. 2010. A framework for assessing

operational model MJO forecasts: a project of the CLIVAR Madden-Julian oscillation working group. *Bulletin of Americal Meteorological Society* .

Hendon HH, Wheeler M, Zhang C. 2007. Seasonal dependence of the MJO-ENSO relationship. *Journal of Climate* **20**: 531–543.

Hoell A, Barlow M, Wheeler MC, Funk C. 2014. Disruptions of El Nino-Southern Oscillation Teleconnections by the MaddenJulian Oscillation. *Geophysical Research Letters* **41**(3): 998–1004.

Hurrell J, Meehl GA, Bader D, Delworth TL, Kirtman B, Wielicki B. 2009. A Unified Modeling Approach to Climate System Prediction. *Bulletin of the American Meteorological Society* **90**(12): 1819–1832.

Jin FF, Lin L, Timmermann A, Zhao J. 2007. Ensemble-mean dynamics of the ENSO recharge oscillator under state-dependent stochastic forcing. *Geophysical Research Letters* **34**.

Juricke S, Jung T. 2014. Influence of stochastic sea ice parametrization on climate and the role of atmosphere-sea ice-ocean interaction. *Philosophical Transactions of the Royal Society a-Mathematical Physical and Engineering Sciences* **372**(2018).

Kim D, Kug JS, Sobel AH. 2013. Propagating vs. Non-propagating Madden-Julian Oscillation Events. *Journal of Climate* **5**: 111–125.

Klingaman NP, Jiang X, Xavier PK, Petch J, Waliser D, Woolnough SJ. 2015. Vertical structure and physical processes of the Madden-Julian oscillation: Synthesis and summary. *Journal of Geophysical Research* **120**(10): 4671–4689.

Kondrashov D, Chekroun MD, Robertson AW, Ghil M. 2013. Low-order stochastic model and "past-noise forecasting" of the Madden-Julian Oscillation. *Geophysical Research Letters* **40**(19): 5305–5310.

Leith CE. 1975. Numerical weather prediction. *Reviews of Geophysics* **13**(3): 681.

Lin H, Brunet G, Derome J. 2008. Forecast skill of the Madden-Julian Oscillation in two Canadian atmospheric models. *Monthly Weather Review* **136**: 4130–4149.

Ling J, Zhang C, Bechtold P. 2013. Large-Scale Distinctions between MJO and Non-MJO Convective Initiation over the Tropical Indian Ocean. *Journal of Atmospheric Sciences* **70**(9): 2696–2712.

Majda AJ, Stechmann SN. 2009. The MaddenJulian oscillation and the multiscale hierarchy of organized convection. *UCLA Tropical Meteorology and Climate Newsletter* .

Majda AJ, Stechmann SN. 2012. Multiscale theories for the MJO. In: *Intraseasonal Variability in the Atmosphere-Ocean Climate System*, Lau WKM, Waliser DE (eds), Springer Berlin Heidelberg: Berlin, Heidelberg, pp. 549–568.

Molteni F, Stockdale T, Balmaseda M, Balsamo G, Buizza R, Ferranti L, Magnusson L, Mogensen K, Palmer T, Vitart F. 2011. The new ECMWF seasonal forecast system (System 4). Technical report, ECMWF.

Moncrieff MW, Shapiro MA, Slingo JM, Molteni F. 2007. Collaborative research at the intersection of weather and climate. *World Meteorological Organization Bulletin* **56**(3).

Moon JY, Wang B, Ha KJ. 2011. ENSO regulation of MJO teleconnection. *Climate Dynamics* **37**(5-6): 1133–1149.

Palmer TN. 2001. A nonlinear dynamical perspective on model error: A proposal for non-local stochastic-dynamic parametrization in weather and climate prediction models. *Quarterly Journal of the Royal Meteorological Society* **127**(572): 279–304.

Palmer TN. 2012. Towards the probabilistic Earth-system simulator: a vision for the future of climate and weather prediction. *Quarterly Journal of the Royal Meteorological Society* **138**(665): 841–861.

Palmer TN, Barkmeijer J, Buizza R, Petroliagis T. 1997. The ECMWF Ensemble Prediction System. *Meteorological Applications* **4**(04): 301–304.

Palmer TN, Buizza R, Doblas-Reyes F, Jung T, Leutbecher M, Shutts G, M S, Weisheimer A. 2009a. Stochastic parametrization and model uncertainty.

Palmer TN, Doblas-Reyes FJ, Weisheimer A. 2009b. Toward seamless prediction: calibration of climate change projections using seasonal forecasts reply.

Palmer TN, Doblas-Reyes FJ, Weisheimer A, Rodwell MJ. 2008. Toward seamless prediction: Calibration of climate change projections using seasonal forecasts. *Bulletin of the American Meteorological Society* **89**(4): 459–470.

Palmer TN, Döring A, Seregin G. 2014. The real butterfly effect. *Nonlinearity* **27**(9): R123–R141.

Palmer TN, Williams PD. 2008. Introduction. Stochastic physics and climate modelling. *Philosophical Transactions of the Royal Society A: Mathematical, Physical and Engineering Sciences* **366**(1875): 2419–2425.

Pegion K, Sardeshmukh PD. 2011. Prospects for Improving Subseasonal Predictions. *Monthly Weather Review* **139**(11): 3648–3666.

Perez CL, Moore AM, Zavala-Garay J, Kleeman R. 2005. A comparison of the influence of additive and multiplicative stochastic forcing on a coupled model of ENSO. *Journal of Climate* **18**: 5066–5085.

Reyes FD, Weisheimer A, Déqué M, Keenlyside N, McVean M, Murphy JM, Rogel P, Smith D, Palmer TN. 2009. Addressing model uncertainty in seasonal and annual dynamical ensemble forecasts. *Quarterly Journal of the Royal Meteorological ...* **135**: 1538–1559.

Robertson AW, Kumar A, Pena M, Vitart F. 2015. Improving and Promoting Subseasonal to Seasonal Prediction. *Bulletin of the American Meteorological Society* **96**: ES49–ES53.

Romine GS, Schwartz CS, Berner J, Fossell KR, Snyder C, Anderson JL, Weisman ML. 2014. Representing forecast error in a convection-permitting ensemble system. *Monthly Weather Review* **142**: 4519–4541.

Roundy PE, MacRitchie K, Asuma J, Melino T. 2010. Modulation of the Global Atmospheric Circulation by Combined Activity in the Madden-Julian Oscillation and the El Nino-Southern Oscillation during Boreal Winter. *Journal of Climate* **23**(15): 4045–4059.

Sanchez C, Williams KD, Collins M. 2015. Improved stochastic physics schemes for global weather and climate models. *Quarterly Journal of the Royal Meteorological Society* **Early Online Release**.

Schneider T, Bischoff T, Haug GH. 2014. Migrations and dynamics of the intertropical convergence zone. *Nature* **513**(7516): 45–53.

Seiffert R, von Storch JS. 2010. A Stochastic Analysis of the Impact of Small-Scale Fluctuations on the Tropospheric Temperature Response to CO2 Doubling. *Journal of Climate* **23**(9): 2307–2319.

Shapiro M, Shukla J, Brunet G, Nobre C, Beland M, Dole R, Trenberth K, Anthes R, Asrar G, Barrie L, Bougeault P, Brasseur G, Burridge D, Busalacchi A, Caughey J, Chen D, Church J, Enomoto T, Hoskins B, Hov O, Laing A, Le Treut H, Marotzke J, McBean G, Meehl G, Miller M, Mills B, Mitchell J, Moncrieff M, Nakazawa T, Olafsson H, Palmer T, Parsons D, Rogers D, Simmons A, Troccoli A, Toth Z, Uccellini L, Velden C, Wallace JM. 2010. An Earth-System Prediction Initiative for the Twenty-First Century. *Bulletin of the American Meteorological Society* **91**(10): 1377–1388.

Shutts G. 2005. A kinetic energy backscatter algorithm for use in ensemble prediction systems. *Quarterly Journal of the Royal Meteorological Society* **131**(612): 3079–3102.

Shutts G, Pallarès AC. 2014. Assessing parametrization uncertainty associated with horizontal resolution in numerical weather prediction models. *Philosophical Transactions of the Royal Society A: Mathematical, Physical and Engineering Sciences* **372**(2018): 20130 284–20130 284.

Shutts GJ, Palmer TN. 2007. Convective forcing fluctuations in a cloud-resolving model: Relevance to the stochastic parameterization problem. *Journal of Climate* **20**(2): 187–202.

Stockdale TN, Anderson DLT, Balmaseda MA, Doblas-Reyes F, Ferranti L, Mogensen K, Palmer TN, Molteni F, Vitart F. 2011. ECMWF seasonal forecast system 3 and its prediction of sea surface temperature. *Climate Dynamics* **37**(3-4): 455–471.

Subramanian AC, Jochum M, Miller AJ, Murtugudde R, Neale RB, Waliser DE. 2011. The Madden-Julian Oscillation in CCSM4. *Journal of Climate* **24**(24): 6261–6282.

Sušelj K, Hogan TF, Teixeira J. 2014. Implementation of a stochastic eddy-diffusivity/mass-flux parameterization into the Navy Global Environmental Model. *Weather and forecasting* **29**(6): 1374–1390.

Suselj K, Teixeira J, Chung D. 2013. A Unified Model for Moist Convective Boundary Layers Based on a Stochastic Eddy-Diffusivity/Mass-Flux Parameterization. *Journal of Atmospheric Sciences* **70**(7): 1929–1953.

Teixeira J, Reynolds CA. 2010. Stochastic Nature of Physical Parameterizations in Ensemble Prediction: A Stochastic Convection Approach. *dx.doi.org* **136**(2): 483–496.

Vitart F. 2014. Evolution of ECMWF sub-seasonal forecast skill scores. *Quarterly Journal of the Royal Meteorological Society* **140**(683): 1889–1899.

Vitart F, Molteni F. 2010. Simulation of the Madden-Julian Oscillation and its teleconnections in the ECMWF forecast system. *Quarterly Journal of the Royal Meteorological Society* **136**(649): 842–855.

Vitart F, Robertson AW. 2012. Subseasonal to Seasonal Prediction Project: bridging the gap between weather and climate. *World Meteorological Organisation Bulletin* **61**(2).

Watson PAG, Christensen HM, Palmer TN. 2015. Does the ECMWF IFS Convection Parameterization with Stochastic Physics Correctly Reproduce Relationships between Convection and the Large-Scale State? *Journal of the Atmospheric Sciences* **72**(1): 236–242.

Weisheimer A, Corti S, Palmer T. 2014. Addressing model error through atmospheric stochastic physical parametrizations: impact on the coupled ECMWF seasonal forecasting system. *Philosophical Transactions of the Royal Society* **372**.

Weisheimer A, Palmer TN. 2014. On the reliability of Seasonal Climate Forecasts. *Journal of the Royal Society Interface* **11**, doi:20131162.

Weisheimer A, Palmer TN, Doblas-Reyes FJ. 2011. Assessment of representations of model uncertainty in monthly and seasonal forecast ensembles. *Geophysical Research Letters* **38**(16).

Williams PD. 2012. Climatic impacts of stochastic fluctuations in air–sea fluxes. *Geophysical Research Letters* **39**(10).

Zavala-Garay J, Zhang C, Moore AM, Wittenberg AT, Harrison MJ, Rosati A, Vialard J, Kleeman R. 2008. Sensitivity of hybrid ENSO models to unresolved atmospheric variability. *Journal of Climate* **21**.

Zhang C. 2005. Madden-julian oscillation. *Reviews of Geophysics* **43**(2).

Zhang C. 2013. Madden-Julian Oscillation: Bridging Weather and Climate. *Bull Am Met Soc* : 1849–1870.

Zhang C, Gottschalck J, Maloney ED, Moncrieff MW, Vitart F, Waliser DE, Wang B, Wheeler MC. 2013. Cracking the MJO nut. *Geophysical Research Letters* **40**(6): 1223–1230.

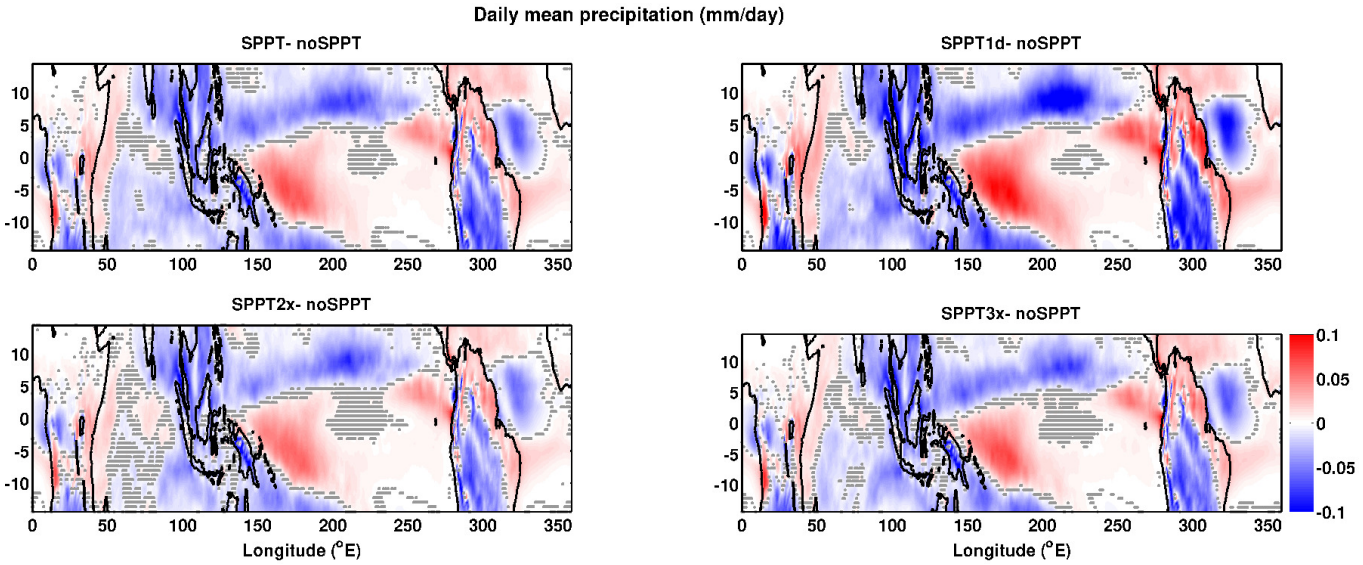

Figure 1. Total daily mean precipitation difference in the Tropics (mm per day) for the months December-January-February. (a) SPPT - noSPPT, (b) SPPT1d - noSPPT, (c) SPPT2x - noSPPT (d) SPPT3x - noSPPT. Regions of no significant differences at the 95% confidence level based on a two-sided t-test are hatched.

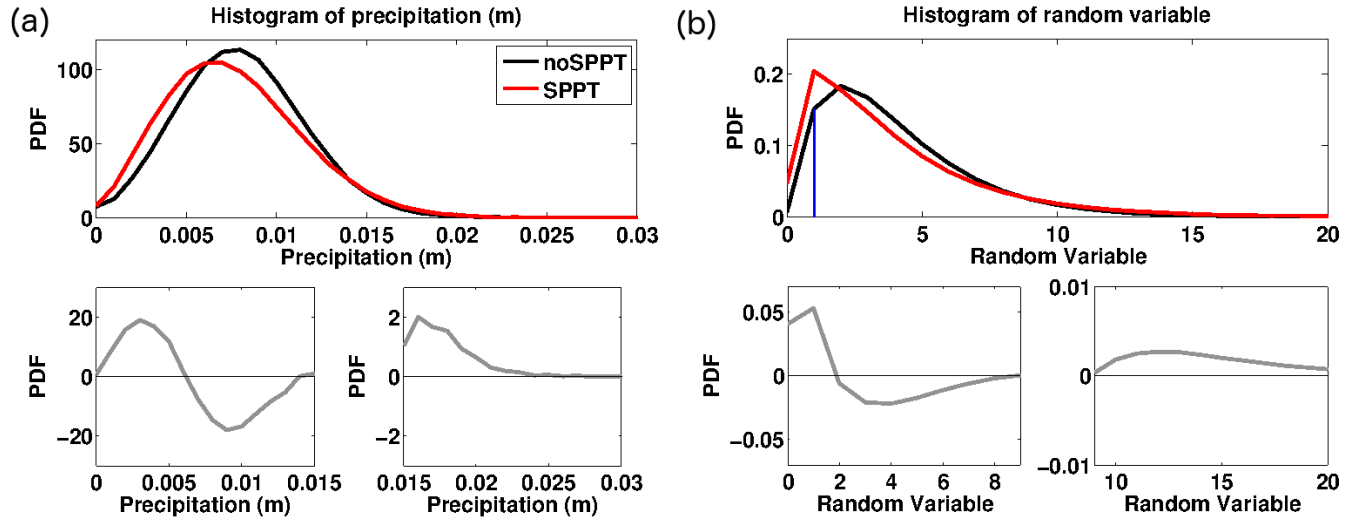

Figure 2. (a) Probability Density Function of precipitation (m) in the West Pacific region (100 °E - 125 °E, 1 °S - 1 °N) for the noSPPT run (black line) and SPPT run (red line). The difference of the two histograms is plotted in the subpanels below in grey. (b) Probability Density Function of a Gamma distributed random variable (black) and the same convolved with the jump-diffusion process (black). The difference of the two histograms is plotted in grey in the subpanels below. The y-axis for the bottom sub-panels are scaled to highlight the magnitude of the differences in the extremes.

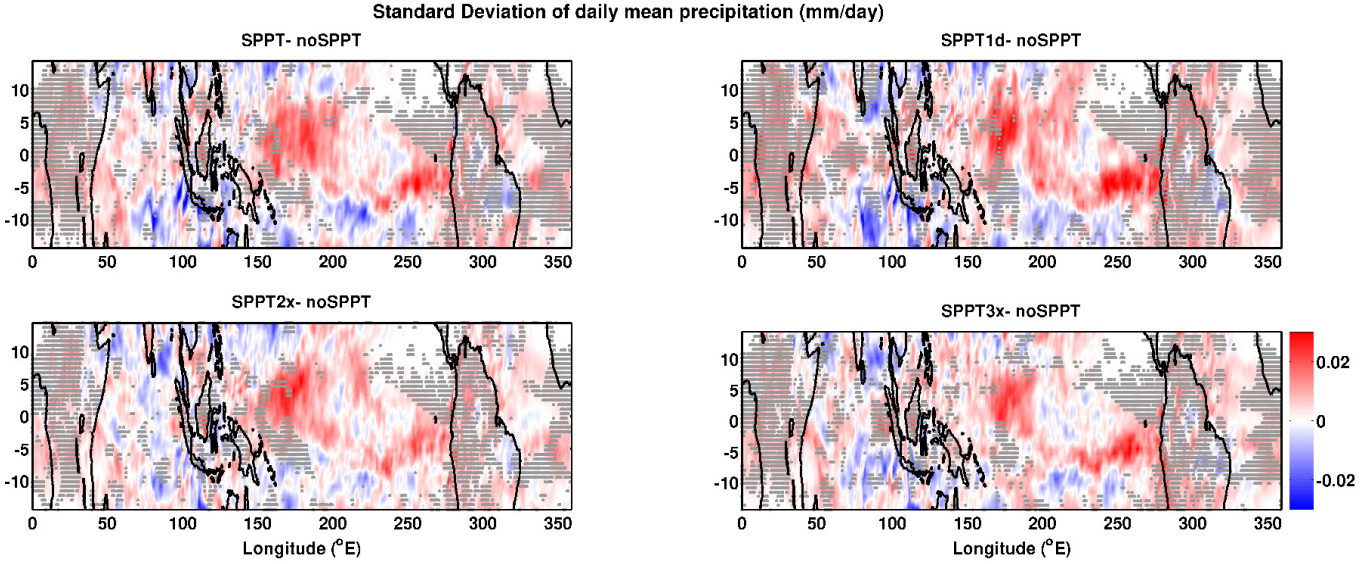

Figure 3. Difference in standard deviation in daily mean precipitation in the Tropics (mm per day) for the months December-January-February. (a) SPPT - noSPPT, (b) SPPT1d - noSPPT, (c) SPPT2x - noSPPT (d) SPPT3x - noSPPT. Regions of no significant differences at the 95% confidence level based on a two-sided t-test are hatched.

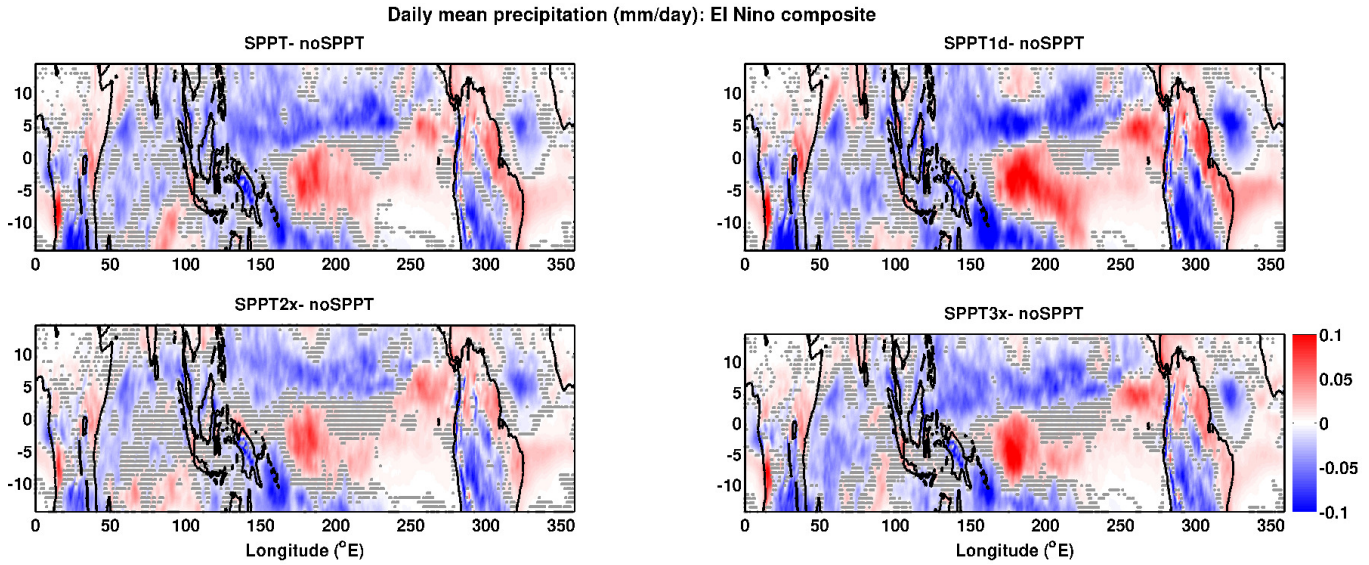

Figure 4. Composite map of total daily mean precipitation difference in the Tropics during El Niño events over the period 1991-2009 for (a) SPPT - noSPPT (b) SPPT1d - noSPPT (c) SPPT2x - noSPPT (d) SPPT3x - noSPPT. Regions of no significant differences at the 95% confidence level based on a two-sided t-test are hatched.

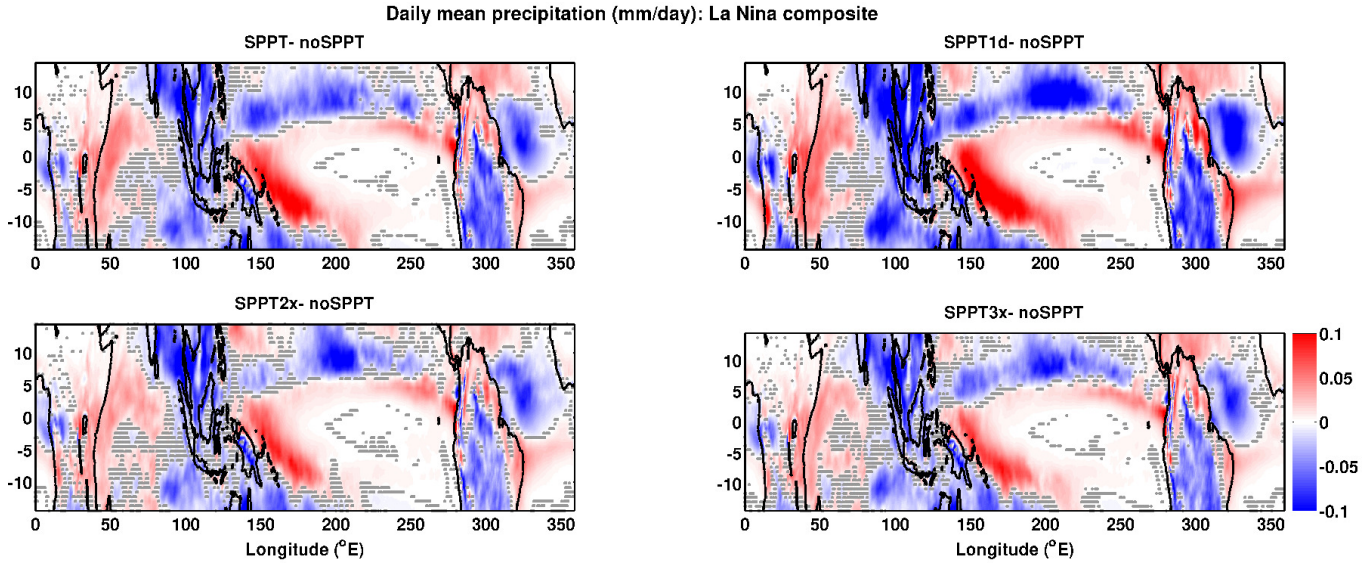

Figure 5. Composite map of total daily mean precipitation difference in the Tropics during La Niña events over the period 1991-2009 for (a) SPPT - noSPPT (b) SPPT1d - noSPPT (c) SPPT2x - noSPPT (d) SPPT3x - noSPPT. Regions of no significant differences at the 95% confidence level based on a two-sided t-test are hatched.

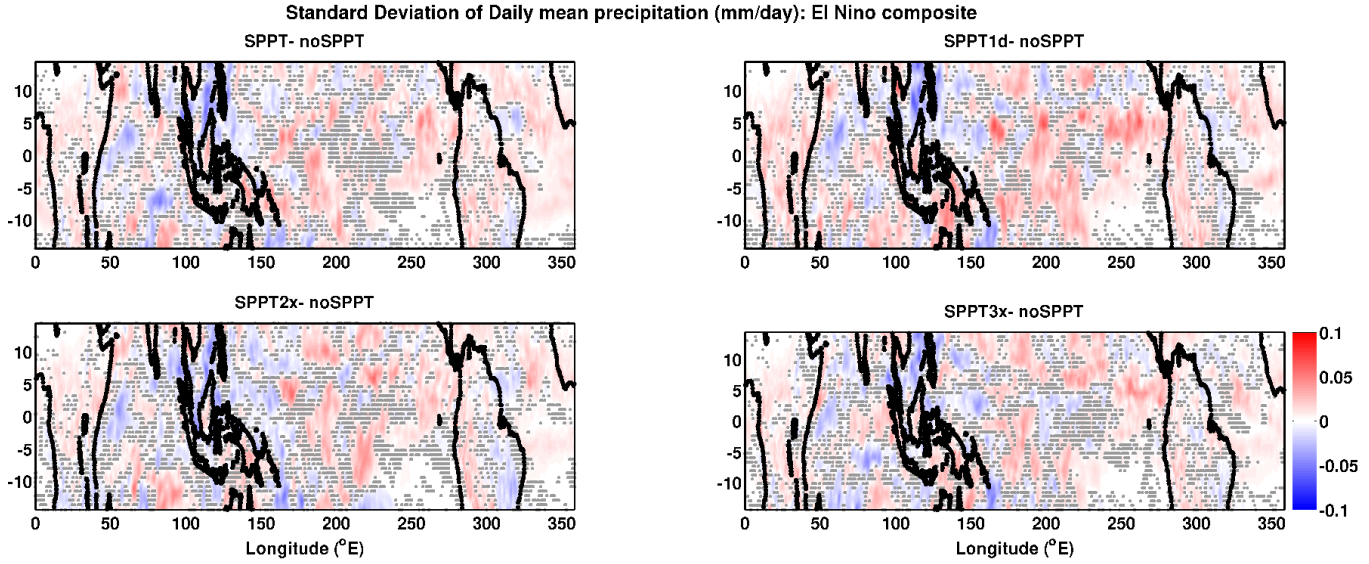

Figure 6. Composite map of difference in ensemble standard deviation of total daily mean precipitation in the Tropics during El Niño events over the period 1991-2009 for (a) SPPT - noSPPT (b) SPPT1d - noSPPT (c) SPPT2x - noSPPT (d) SPPT3x - noSPPT. Regions of no significant differences at the 95% confidence level based on a two-sided t-test are hatched.

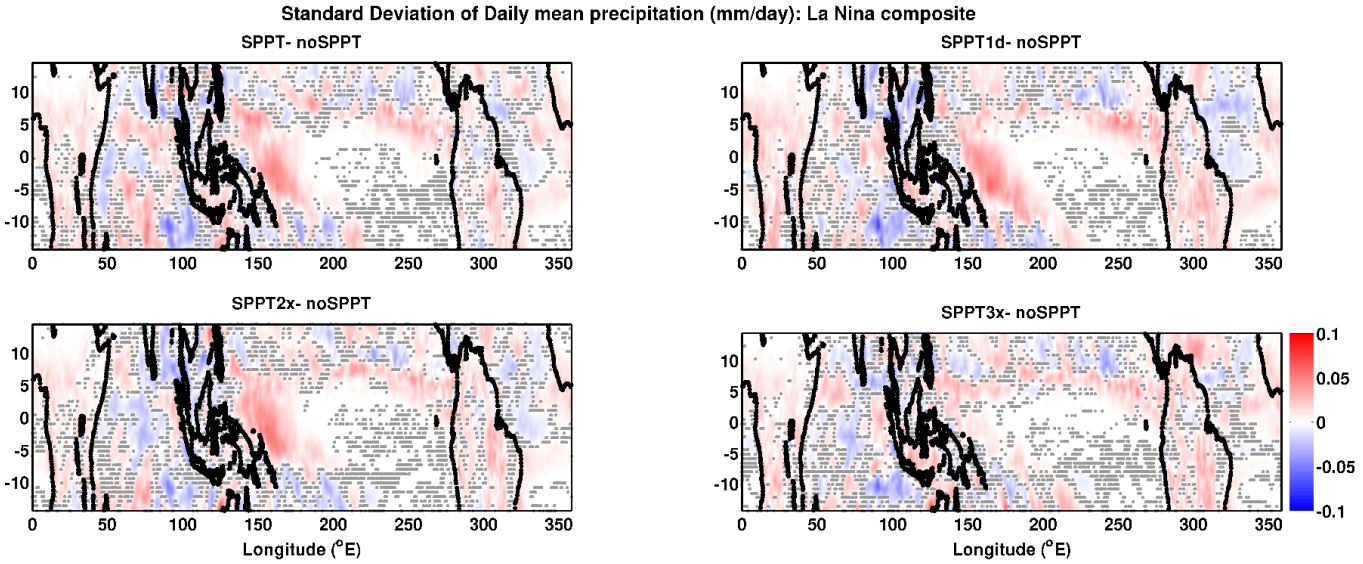

Figure 7. Composite map of difference in ensemble standard deviation of total daily mean precipitation in the Tropics during La Niña events over the period 1991-2009 for (a) SPPT - noSPPT (b) SPPT1d - noSPPT (c) SPPT2x - noSPPT (d) SPPT3x - noSPPT. Regions of no significant differences at the 95% confidence level based on a two-sided t-test are hatched.

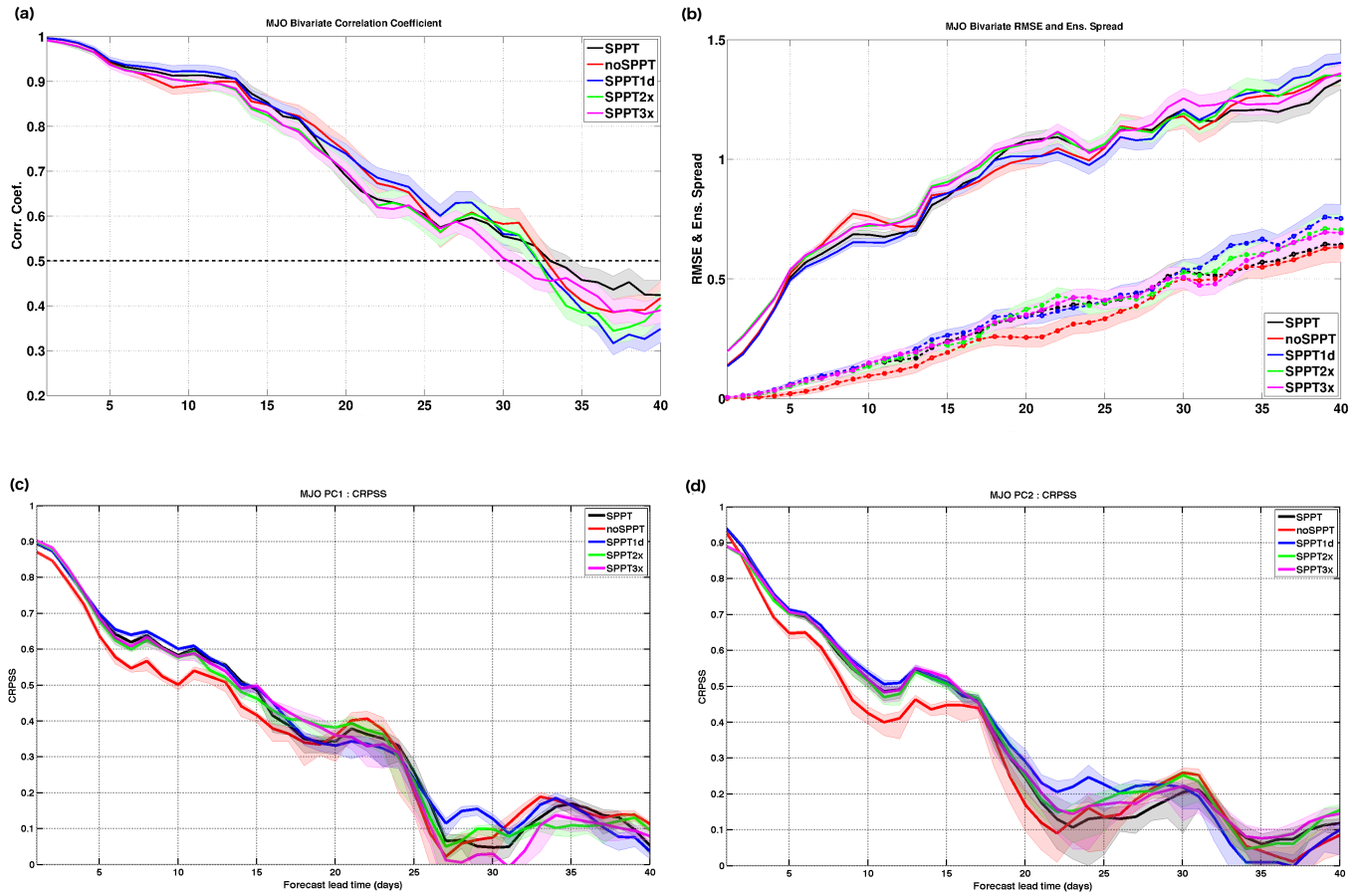

Figure 8. (a) Bi-variate correlations with lead time of hindcast and observed RMM1 and RMM2, for the different SPPT sensitivity experiments. The horizontal line represents a correlation skill of 0.5. The shaded regions represent the 95% confidence interval computed using a 10,000 bootstrap re-sampling procedure, (b) Root Mean Square error (continuous lines) and ensemble spread (dashed lines) with lead time of hindcast and observed RMM1 and RMM2, for the different sensitivity experiments. The shaded region represent the 95% confidence interval computed using a 10,000 bootstrap re-sampling procedure. The ranked probability skill scores of the ensemble mean (c) RMM1 and (d) RMM2 computed for the different experiments. The shaded region represents the confidence intervals using a bootstrap re-sampling technique.

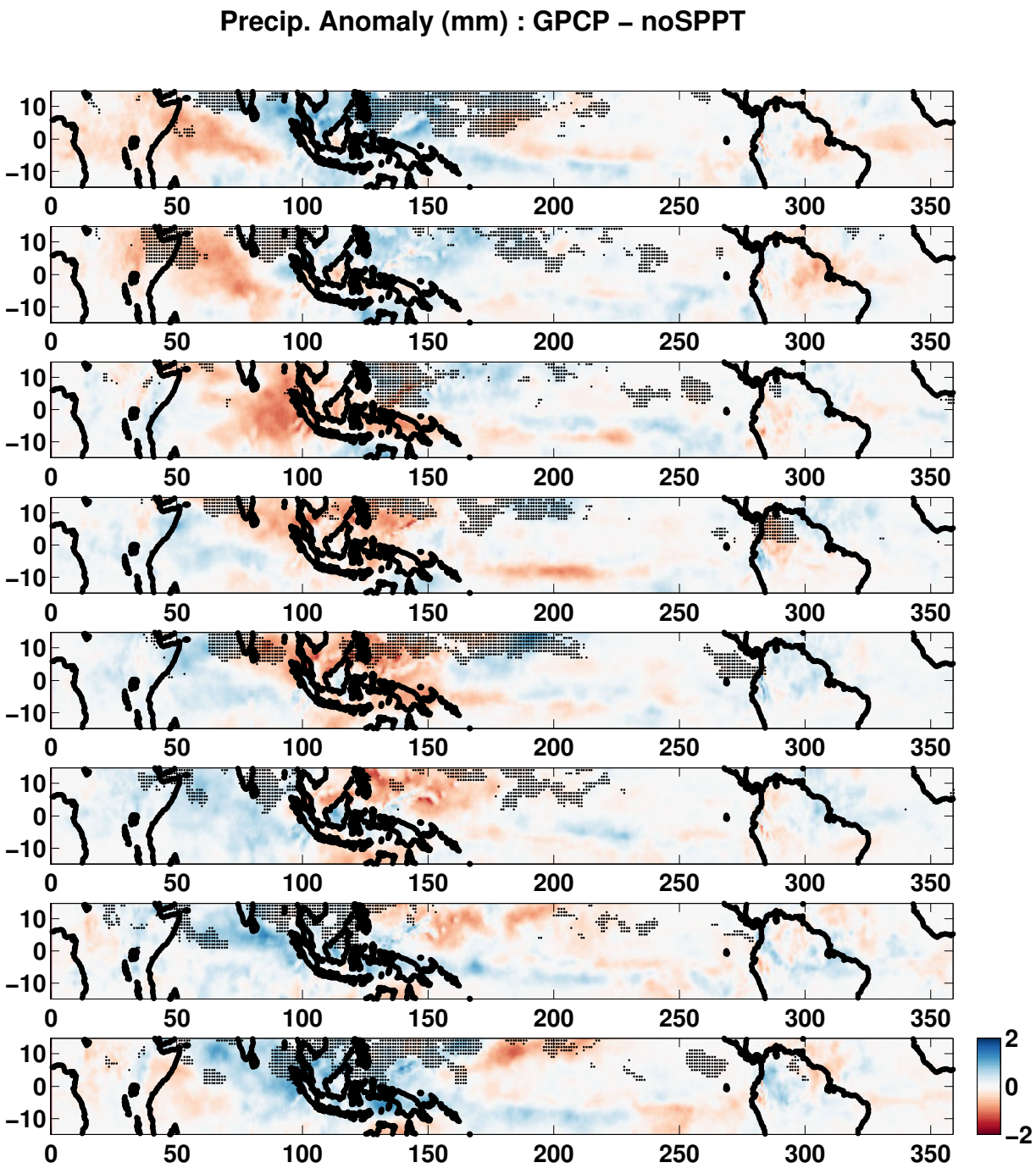

Figure 9. Composite maps of precipitation anomaly difference between the noSPPT experiment and the GPCP observed precipitation anomaly during the 8 phases of the MJO. Composites are built for the MJO events in 15 ensembles for 20 years when the MJO amplitude is greater than 1 in the corresponding phases for each of the experiments. Regions of significant differences at the 95% confidence level based on a two-sided t-test are not hatched.

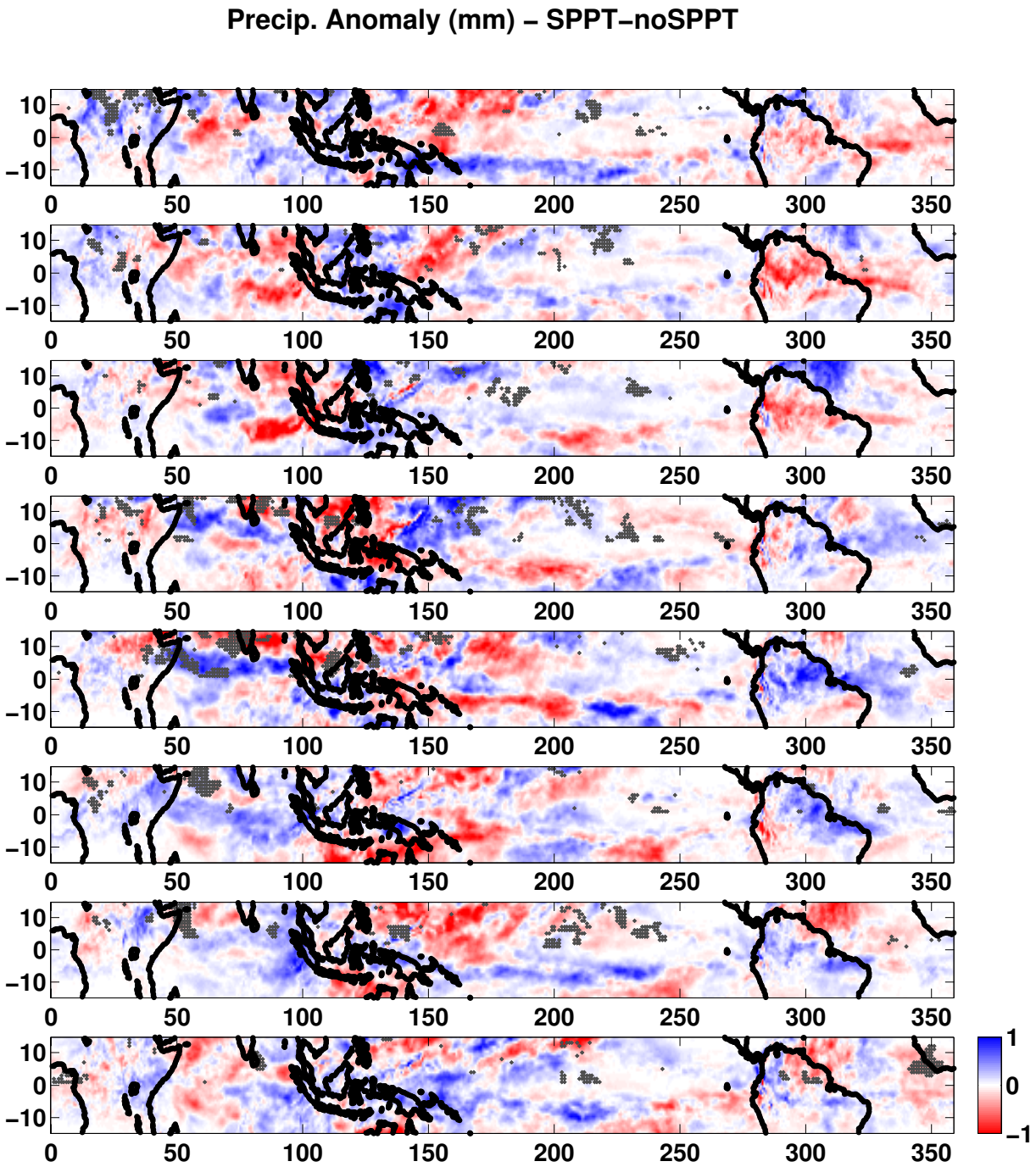

Figure 10. Composite maps of precipitation anomaly difference between the SPPT and noSPPT experiments during the 8 phases of the MJO. Composites are built for the MJO events in 15 ensembles for 20 years when the MJO amplitude is greater than 1 in the corresponding phases. Regions of significant differences at the 95% confidence level based on a two-sided t-test are not hatched.

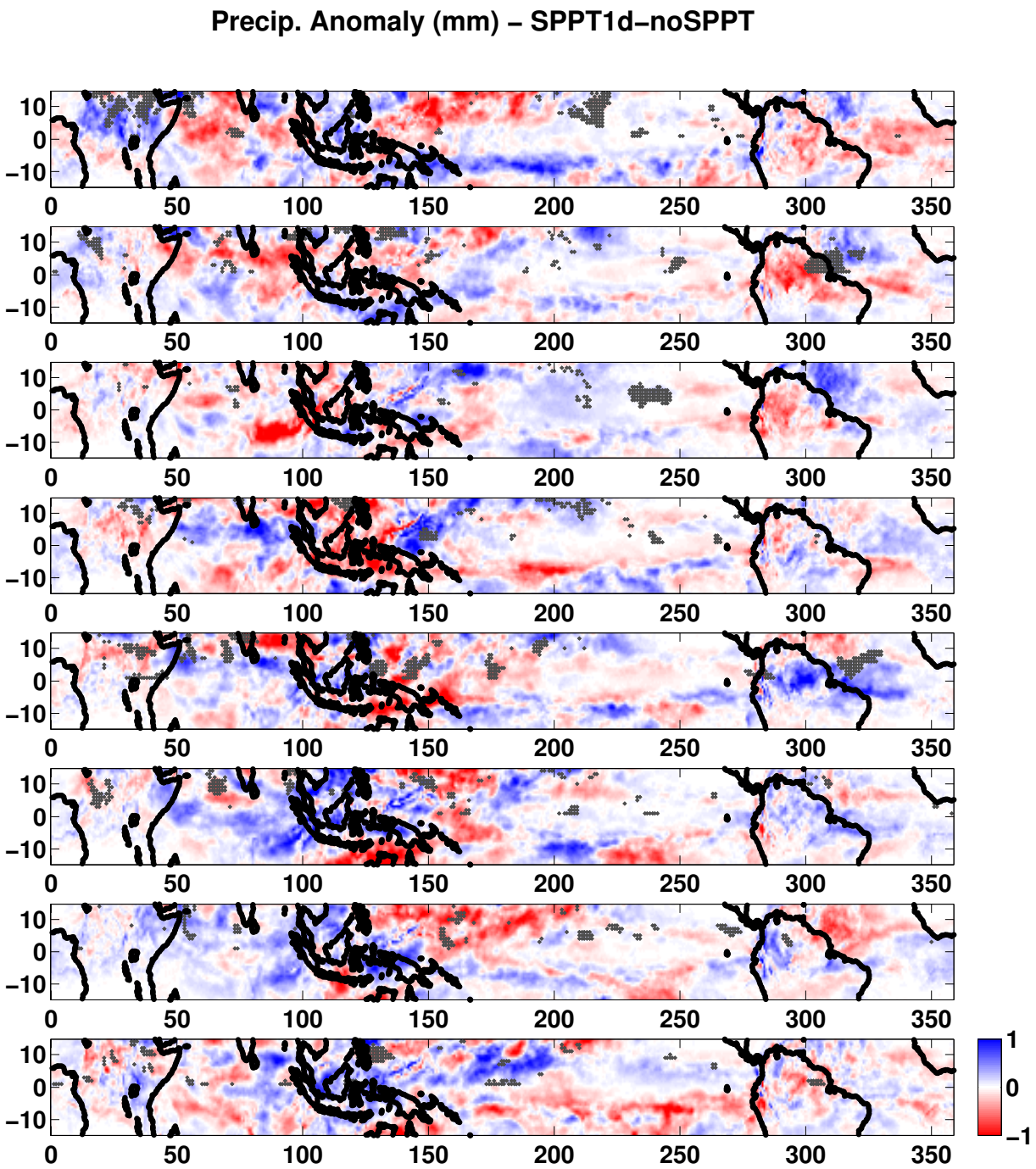

Figure 11. Composite maps of precipitation anomaly difference between the SPPT1d and noSPPT experiments during the 8 phases of the MJO. Composites are built for the MJO events in 15 ensembles for 20 years when the MJO amplitude is greater than 1 in the corresponding phases. Regions of significant differences at the 95% confidence level based on a two-sided t-test are not hatched.